10-18-2016

Radiation Fog Chemical Composition and Its Temporal Trend Over an Eight Year Period

Derek J. Straub
Susquehanna University

Radiation fog chemical composition and its temporal trend over an eight year period

Derek J. Straub[a,1]

[a]Department of Earth and Environmental Sciences, Susquehanna University, 514 University Avenue, Selinsgrove, PA 17870 USA
straubd@susqu.edu

[1]Corresponding Author: Department of Earth and Environmental Sciences, Susquehanna University, 514 University Avenue, Selinsgrove, PA 17870 USA
straubd@susqu.edu, Phone: 570-372-4767, Fax: 570-372-2752

Abstract

Radiation fog samples have been collected at a rural site in Central Pennsylvania from 2007 through 2015 in order to document chemical composition, assess concentration changes over time, and to provide insight into emission sources that influence the region. The collection of samples over multiple years makes this one of the few long duration radiation fog studies that have been completed. During the course of the campaign, 146 samples were obtained and analyzed for pH, major inorganic ions, low molecular weight organic acids, total organic carbon (TOC) and total nitrogen (TN). Ammonium (median concentration = 209 μN), sulfate (69 μN), calcium (51 μN), and nitrate (31 μN) were the most abundant inorganic ions, although these were present at much lower concentrations than for radiation fog studies conducted in other locations. Organic acids, of which formate (20 μM) and acetate (21 μM) were the most abundant, were closer in magnitude to measurements made during previous studies. Organic acids accounted for 15% of TOC, which had a median concentration of 6.6 mgC l^{-1}. The median concentration of TN was 3.6 mgN l^{-1}, 18% of which was determined to be organic nitrogen. Statistically significant decreasing trends from 2007 to 2015 were noted for sulfate, ammonium, chloride, and nitrate. For the same period, an increase in pH was observed. Seasonal trends were identified for a number of species as well. The partitioning of ammonia between the gas and aqueous phases was also investigated and found to deviate significantly from equilibrium.

Keywords: radiation fog chemistry; organic acids; total organic carbon; total nitrogen; multi-year trends; ammonia partitioning

1. Introduction

In the Northeastern United States, radiation fog formation is a relatively common occurrence during the fall when nights become longer, skies are clear, and winds are calm. These conditions tend to promote strong radiational cooling at the surface which can lead to saturation in the surface layer and fog droplet formation. The turbulent transfer of heat and water vapor are also critical factors in the initial formation and maintenance of radiation fogs (Degefie et al., 2015; Liu et al., 2011; Gultepe et al., 2007). Topography may enhance fog development and influence its spatial extent such as when radiatively cooled air accumulates at the bottom of river valleys. The term air-drainage fog has been used to classify this subcategory of radiation fogs (George, 1951). This often occurs in the Northeastern US when radiation fog preferentially forms in the deeper river valleys, producing a dendritic appearance on visible satellite imagery. In the presence of a large high pressure system, radiation fog can be observed in the river valleys extending from West Virginia to New Hampshire, including many of the valleys in the Ridge and Valley region of Pennsylvania.

It has long been recognized that fog droplets interact with aerosol particles and soluble gases in the atmosphere. Fog droplets scavenge, modify through chemical and physical processes, redistribute, and remove from the atmosphere both particles and gases. Because fogs affect pollutant formation, transformation, and removal, they have been the subject of field and laboratory research over the years. Recent examples of field-based radiation fog research include the documentation of fog composition and identification of pollutant sources (Li et al., 2011; Błas et al., 2010; Raja et al., 2008), the effect of droplet size on composition and the production of inorganic aerosol mass (Fahey et al., 2005; Moore et

al., 2004a; 2004b; Reilly et al., 2001), the removal of trace species from the atmosphere (Herckes et al., 2007; Burkard et al., 2003; Collett et al., 2001), scavenging efficiencies (Gilardoni et al., 2014), organic nitrogen speciation and processing (Wang et al., 2015; Zang and Anastasio, 2003a; 2003b; McGregor and Anastasio, 2001), organic carbon speciation and processing (Herckes et al., 2013; Ervens et al., 2013; Ehrenhauser et al., 2012; Raja et al., 2009; Collett et al., 2008; Fuzzi et al., 2002), and secondary particle formation (Kaul et al., 2011; Dall'Osto et al., 2009). Nearly all radiation fog field campaigns are short term, intensive studies with samples obtained during a limited number of events.

Because fog droplets have been shown to be effective scavengers of aerosol particles and trace gases, they can provide an indication of local or regional air quality and can reveal changes over time if sampling occurs over an extended period. There have been a number of multi-year cloud water studies at high elevation sites to compile long-term cloud water composition data or to quantify monthly, seasonal, or yearly trends (Yamaguchi et al., 2015; Deguillaume et al., 2014; Gioda et al., 2013; Murray et al., 2013; Vaitilingom et al., 2012; Aleksic et al., 2009; Aikawa et al., 2007; Anderson et al., 2006; Tago et al., 2006; Baumgardner et al., 2003; Anderson et al., 1999; Acker et al., 1995; Schemenauer et al., 1995; Mohnen and Kadlecek, 1989). In most of these studies stratus, frontal, or orographically enhanced clouds were targeted. In comparison to cloud studies, long term sampling of radiation fog has been limited to only a few locations. Studies with sufficiently long data sets to evaluate trends have only been published for sites in Strasburg, France, the Po Valley in Italy, and the Central Valley in California. A ten year record of radiation fog composition was obtained in Strasburg to examine temporal trends in major ions and trace metals (Herckes et al., 2002a). In the Po Valley, short term studies of radiation fog began in the early 1980's, with more systematic sampling beginning in 1989 at the San Pietro Capofiume field site. Trends in inorganic ions, organic acids, and water soluble organic carbon observed over a 20 year period have recently been published for that location (Giulianelli et al., 2014). Radiation fog sampling in the Central Valley of California has taken the form of individual intensive field campaigns,

but these have occurred fairly regularly at various sites in the Valley since 1982. Herckes et al. (2015) published a compilation of results from studies over a 30 year period with a focus on spatial variations and temporal trends in fog occurrence and composition.

In addition to these three sites, radiation fog composition measured over a multi-year period is now available for a site in the Mid-Atlantic region of the United States. Sample collection began in 2007 on the campus of Susquehanna University, located in the Ridge and Valley Region of Central Pennsylvania. Through 2015, 146 fog events have been sampled and analyzed with the objectives of documenting radiation fog composition in the region and identifying trends over time. The results presented in this paper build on the initial findings of inorganic ion composition at this location (Straub et al., 2012), and now includes measurements of low molecular weight organic acids, total organic carbon (TOC), and total nitrogen (TN). A sufficiently long data record is also now available to present temporal trends.

2. Methods

2.1 Sampling Location

Fog sampling occurred during an eight year period from 2007 through 2015 at the Center for Environmental Education and Research (CEER) on the campus of Susquehanna University in Central Pennsylvania. The sampling site was located 3 km from the Susquehanna River and is immediately surrounded by land used for agricultural purposes. Local emission sources include two uncontrolled coal combustion units, a 400 MW coal-fired electrical generation plant 7 km to the Northeast and a much smaller coal-fired steam plant 1.3 km to the East. Both of these facilities were decommissioned in early 2014. In addition, this area is influenced by agricultural emissions derived from fertilizer application and livestock. Transportation, home heating, and industry sources are also present at a level consistent with a rural area.

Climatologically, the sampling location experiences 25 to 30 days with dense fog per year, defined as having visibility less than or equal to 0.25 miles (NOAA, 2002). The vast majority of the fog events are radiation fogs that occur any time between May and November, but are most common in the fall. Though infrequent, this area also experiences occasional fog development associated with precipitation or as a result of warm air advection from the south when snow cover is present. For the purposes of this study, a fog event was classified as a radiation fog if wind speeds were less than 2.5 m s^{-1} and skies were clear or mostly clear in the hours immediately prior to sample collection. Events in which rain occurred during the sample collection period were considered precipitation fogs and were not included in this study. Because the sampling equipment was not actively maintained during the winter months, no advection fog samples were collected.

2.2 Sample Collection

Fog samples were collected throughout the study period with a Caltech Heated Rod Cloud Collector (CHRCC) mounted 2 m above the ground. The CHRCC contained six rows of 3.2 mm diameter stainless steel rods which act as impaction surfaces. The rods were oriented at a 35° angle to the vertical and were mounted in a Teflon trough at the base. Air and fog droplets were drawn into the collector and past the collection rods at a flow rate of 5.6 m^3 min^{-1} by a fan located in the rear of the collector. After impaction, the accumulated cloud droplets flowed down the rods, through the Teflon trough, and into a collection bottle. The combination of droplet velocity and impaction rod diameter produced a theoretical 50% cut-off diameter of 9 microns (Demoz et al., 1996).

The system was automated with a fog detector and pneumatically actuated front and rear doors. The presence of fog was initially detected with a Colorado State University Optical Fog Detector (CSU-OFD; Carrillo et al., 2008). In 2010 the CSU-OFD was replaced with a Belfort model 3100 visibility monitor which reduced sensitivity to precipitation and improved reliability. The collection system was

activated when threshold values reached 60 mg m^{-3} when the CSU-OFD was in use or 500 m for the visibility sensor. A single bulk sample was obtained during each fog event.

The sampler was washed thoroughly with 18 MΩ deionized (DI) water whenever a fog event was expected or at least once per week to ensure that the collector was clean in case of unexpected fog formation. After washing, a blank sample was obtained by spraying DI water into the inlet and allowing it to drain from the collection rods into the sample bottle. Every blank sample that immediately preceded a fog event was analyzed along with the sample to verify that the collector was uncontaminated. In addition, the blank samples were used for the calculation of detection limits.

Through 2015, 146 fog events were sampled. A single radiation fog sample was obtained in 2007 when the program first began. An average of 12 samples were collected per year from 2008 through 2010. The rate of sampled fog events increased to an average of 22 per year from 2011 to 2015 primarily due to the increased reliability of the Belfort visibility monitor to detect fog and activate the system.

In 2012 a leak was discovered in the collector at the location where the impaction rods penetrate the Teflon trough that funnels accumulated fog droplets into the sample bottle. The press-fit connections between the impaction rods and the Teflon trough either loosened over time or perhaps did not seal perfectly from the beginning of the project. The result is that some of the accumulated fog water was lost before it reached the sample bottle. This sample loss reduced the overall collected volume, but should not have affected measured concentrations. Because the collector was automated and ran unattended, the leak was not discovered sooner. Unfortunately, it was not possible to determine how long the leak occurred or the volume of sample that was lost. The leak was corrected before the 2013 fog season. Liquid water content (LWC) data are therefore only available for 2008 and 2009 when the CSU-OFD was in use and calibrated for direct LWC measurement, and for the period

2013 – 2015 after the leak was fixed and estimates could be based on collected sample volume, air flow rate, and CHRCC efficiency (Demoz et al., 1996).

2.3 Sample Analysis

After each fog event, the collected sample was weighed and its pH was measured using an Accumet AR50 pH meter calibrated against pH 4.0 and pH 7.0 buffers. Samples were then prepared for inorganic ion, organic acid, TOC, and TN analyses. Samples for major ion and organic acid analyses were stored at 4°C while samples for TOC and TN analyses were frozen until measurements were made. Samples for organic acid analysis were preserved by adding chloroform to make a 2.5% solution. Major inorganic ions were quantified from the beginning of the field project in 2007; however, some of the samples collected in 2008 were prioritized for other studies and inorganic ions were not measured in every sample that year. The analysis of organic acids began in 2012 while the analysis of TOC and TN both began in 2013. The number of samples analyzed for each species can be found in Table 1.

Inorganic ions and organic acids were analyzed by ion chromatography (IC) using a Dionex ICS-2000 system with suppressed conductivity detection. For anions (Cl^-, SO_4^{2-}, and NO_3^-), an AS12A analytical column with carbonate/bicarbonate eluent was used prior to 2009 and an AS18 column and KOH eluent was used thereafter. Cations (Na^+, NH_4^+, K^+, Mg^{2+}, Ca^{2+}) were quantified with a CS12A column and methanesulfonic acid (MSA) eluent. Separation of organic acids (acetate, propionate, formate, methanesulfonate, pyruvate, valerate, glutarate, succinate, maleate, and oxalate) was performed with an AS11 column and a gradient KOH elution. This method measures the total of the ionic and non-ionic forms of each organic acid present in the sample. In addition to organic acids, the AS11 column was used to measure several additional inorganic anions (F^-, NO_2^-, PO_4^{3-}).

When sufficient sample volume was available, TOC was analyzed with a Shimadzu TOC analyzer (TOC-L) which directly measures total carbon and inorganic carbon, with TOC being the difference

between the two. The TOC-L was calibrated against potassium hydrogen phthalate and sodium carbonate/bicarbonate standards. Because organic carbon could have either been dissolved in the fog samples or present in the form of insoluble particles, a number of samples were used to determine the fraction of dissolved organic carbon (DOC). An additional analysis was performed for 12 events in which a portion of the sample was filtered (0.2 µm PTFE membrane) to exclude any insoluble particles and therefore provide a measure of DOC. The Shimadzu TOC-L was also equipped with a total nitrogen module (TNM-L) which was used when sufficient sample remained after TOC analysis. The TNM-L was calibrated against potassium nitrate standards.

Detection limits (DL) at the 95% confidence level for the IC analyses were calculated from the field blanks that were obtained before the collection of each sample over the duration of the campaign (Table 1). While the majority of ions were measured at levels greater than the detection limits, sodium was found to be below the detection limit in approximately 80% of samples. Other inorganic ions measured below the detection limit were potassium (4 samples), magnesium (17), and fluoride (20). Organic acids, with the exception of acetate and formate, were present at levels below the detection limit in many samples as illustrated graphically in Figure 1. When a measurement was below the detection limit, a value of one-half the detection limit was used for the purposes of calculating averages. Detection limits for TOC were also based on field blanks while detection limits for TN were determined from replicate analyses of the lowest concentration standard. TOC and TN values exceeded the detection limits for all samples.

Analytical precision calculations were based on replicate measurements of standards that were made during each IC run throughout the campaign. Precision is presented as relative standard deviations (RSD) in Table 1. The accuracy of the IC analyses for inorganic ions was checked by analyzing NIST traceable standards along with the samples and blanks during every IC run. Measurements of the NIST traceable standards were within ±7% of the certified values on average for magnesium, chloride,

and phosphate and within ±4% of the certified values on average for the remaining ions. NIST traceable check standards were not available for other species.

3. Results and Discussion

Late summer and early fall are meteorologically favorable for radiation fog formation in the study region. As a result, about 75% of the samples were collected during the months of August, September, and October. Approximately 20% were collected in May and June, while only a few samples were collected during the months of April, July, and November. The average start time was 3:30 AM and the average sample duration was just under 4 hours, through there was a great deal of variability in collection times and durations.

3.1 Fog Composition

Inorganic ion composition was dominated by ammonium (median concentration = 209 μN) which is not uncommon in agricultural regions where emissions of ammonia from fertilizer application and livestock can be extensive. Ammonium was followed by sulfate (69 μN), calcium (51 μN), nitrate (31 μN), and bicarbonate (22 μN), which was assumed to be in equilibrium with gas phase CO_2 at the measured fog pH and temperature. The remaining inorganic ions all had median concentrations less than 10 μN (Table 1).

Acetate (median concentration = 21 μM) and formate (20 μM) were the most abundant organic acids that were measured, as is the case in most aqueous and gas phase studies (Chebbi and Carlier, 1996). The next two most abundant organic acids, propionate and oxalate, were observed at median concentrations a factor of ten lower. The remaining organic acid ions had median values that ranged between 0.1 and 1 μM (Figure 1).

The median TOC concentration, measured in 67 samples, was 6.6 mgC l^{-1}. In 12 of those samples, DOC was also determined. For those samples in which both were measured, there was good agreement (r = 0.98) between TOC and DOC. The majority of the organic carbon in these samples was found to be water soluble. DOC accounted for 82 ± 8% of TOC (Figure 2), similar to values reported by others. In bulk radiation fog samples collected in the Central Valley of California, DOC fractions of 76% and 84% were calculated for fog samples collected in Fresno (Collett et al., 2008) and Angiola (Herckes et al., 2013). Additional observations of DOC fractions in radiation fog include 89% along the US Gulf Coast (Raja et al., 2008), 86% and 87% in the Po Valley, Italy (Giulianelli et al., 2014; Facchini et al., 1999), and 95% in Dubendorf, Switzerland (Capal et al., 1990).

For the 59 samples in which organic acids and TOC were both analyzed, the measured organic acids accounted for only a small fraction of TOC. In aggregate they contributed an average of 15% (range: 3% to 37%) to TOC based on carbon mass, while the balance of TOC remained unspeciated. Individual contributions to TOC from acetate, formate, maleate, and propionate were 7.0%, 2.9%, 2.3%, and 1.3% respectively. The remaining organic acids added less than 1% each to TOC. These observations are consistent in magnitude to other radiation fog studies that have investigated organic composition (Collett et al., 2008; Collett et al., 1999; Herckes et al., 2002b; Herckes et al., 2002c).

Overall, organic and inorganic species contributed nearly evenly to the total solute mass loading. When TOC was converted to organic mass using a factor of 1.8, organic matter accounted for 52% of solute mass when averaged over the 61 samples with inorganic ions and TOC values available. However, the contribution of organic matter to total solute mass was quite variable, ranging from 24% to 80%. The average split between organic and inorganic mass noted here is higher than values reported for other radiation fog studies. In the Central Valley of California, Herckes et al. (2007) calculated that organic mass accounted for 29% total solute mass, while Collett et al. (2008) arrived at a value of

approximately one-third of total solute mass. In the Po Valley, 25% of the total solute mass was found to be organic (Giulianelli et al., 2014) and along the Gulf Coast the value was 13% (Raja et al., 2005).

TN was measured in 55 samples from 2013 through 2015. TN analysis was based on unfiltered samples; however, filtered samples (0.2 µm PTFE membrane) were analyzed in parallel on 12 occasions. The results showed that the filtered and unfiltered concentrations agreed within 0.3% on average, suggesting that total nitrogen was essentially completely dissolved. The median TN value was 3.6 mgN l^{-1}, with inorganic nitrogen accounting for the majority of that value. Ammonium, nitrate, and nitrite contributed 67%, 11%, and 4% of the measured TN on average. Organic nitrogen made up the remaining 18% of TN. Measurements of TN and organic nitrogen in radiation fog samples are relatively rare, but the partitioning of TN observed during this study is similar to two radiation fog studies conducted in the Central Valley of California. In those studies, organic nitrogen accounted for 16% of TN in Davis (Zhang and Anastasio, 2001) and between 10% and 17% in Fresno (Collett et al., 2008). While the fractions of organic nitrogen were similar among the radiation fog studies, the absolute concentrations of organic nitrogen were quite different. Compared to this study, organic nitrogen concentrations were greater by a factor of three in Fresno and by a factor of 10 in Davis.

A wide range of pH values was observed during this study, from 3.08 to 7.41. The average pH, based on average H^+ concentration, was 4.65 and the median value was 6.46. The majority of samples had a pH value that fell between 6.0 and 7.0, though a secondary peak in the pH distribution was present between 4.5 and 5.0 pH units (Figure 3). Figure 3 also shows the contribution of species that typically have the greatest impact on pH values: inorganic acids (sulfate and nitrate), organic acids (acetate and formate), and neutralizing species (ammonium and calcium). For samples with the lowest pH values (<4.5), organic acids appear to have been the primary acidifying species rather than sulfate and nitrate. Unfortunately, no specific meteorological conditions or emission sources have yet been identified that account for these elevated organic acid concentrations or the increase in the frequency

of samples in the 4.0 to 5.0 pH range. At pH values above about 5, the fraction of inorganic acids began to exceed that of organic acids. At that point, however, the fraction of both generally decreased in the presence of abundant neutralizing species. The substantial amount of ammonium in the fog samples resulted in high pH values in the majority of samples. Neutralization by carbonate species can also be inferred in samples with high calcium concentrations, which occasionally exceeded concentrations of ammonium.

3.2 Charge balance

A charge balance between anions and cations is often used as an indicator of data quality in fog studies. An equal number of positive and negative charges in an individual sample ($\Sigma_{anions}/\Sigma_{cations} = 1$) indicates that electroneutrality is satisfied, that the majority of charged species were measured, and that analytical and other errors were minimized. For samples collected prior to 2012 in which organic acids were not measured, the average charge balance was 0.64. For samples collected during 2012 and later, measurements of organic acids, nitrite, phosphate, and fluoride were available and were included in the charge balance, resulting in an average value of 0.81. For this calculation, only the fraction of the organic acids in their ionic forms, determined as a function of sample pH, were considered. While the inclusion of these additional anions brings the charge balance closer to unity, an anion deficit still exits.

When evaluating the charge balance as a function of pH, it became clear that the lowest charge balance ratios were associated with higher pH values. For samples with a pH less than 6.0, the charge balance averaged 1.00 ± 0.10 while samples with a pH greater than 6.0 had an average charge balance of 0.74 ± 0.12. This observation led to a focus on bicarbonate, which rapidly becomes the dominant form of inorganic carbon at pH values above 6.3, and was the only species included in the charge balance that was not explicitly measured. Instead, the aqueous phase bicarbonate concentration

($[HCO_3^-]_{aq}$) was assumed to be in equilibrium with gas phase CO_2 (p_{CO_2}) at the measured fog pH and temperature:

$$[HCO_3^-]_{aq} = \frac{H_{CO_2} K_{a1} p_{CO_2}}{[H^+]} \quad \text{(Eqn. 1)}$$

Where H_{CO_2} is the Henry's law coefficient for CO_2, K_{a1} is the dissociation constant for dissolved CO_2, and $[H^+]$ is the aqueous phase hydrogen ion concentration.

Numerous studies have investigated gas/liquid phase partitioning in clouds and fogs, with nearly all showing significant discrepancies, both supersaturation and subsaturation, between measured aqueous concentrations and expected concentrations based on Henry's law equilibrium with the gas phase (Acker et al., 2008; Moore et al., 2004b; Sellegri et al., 2003; Jaeschke et al., 1998; Laj et al., 1997; Winiwarter et al., 1994; Facchini et al., 1992a; 1992b; Winiwarter et al., 1992; Pandis and Seinfeld, 1991; Winiwarter et al., 1988; Jacob et al., 1986). These studies have shown that deviations from equilibrium can result from mixing of droplets that are individually in equilibrium with the gas phase, variations in liquid water content over the course of the sampling period, mass transfer limitations, or some combination of these phenomena.

To investigate further, a second method of determining bicarbonate concentrations was considered. Inorganic carbon concentrations were available for a subset of samples that underwent TOC analysis. To determine bicarbonate concentrations from these measurements, sample pH was used to partition inorganic carbon into dissolved carbon dioxide, bicarbonate, and carbonate. Following the procedure of Seinfeld and Pandis (2006), the molar fraction of bicarbonate was calculated as:

$$\frac{[HCO_3^-]_{aq}}{[CO_2^T]} = \left(1 + \frac{[H^+]}{K_{a1}} + \frac{K_{a2}}{[H^+]}\right)^{-1} \quad \text{(Eqn. 2)}$$

Where K_{a2} is the dissociation constant for bicarbonate and $[CO_2^T]$ is the total CO_2 in solution, here assumed to be equal to the inorganic carbon concentration from the TOC analysis. A similar calculation indicated that carbonate concentrations were negligible for the fog pH values in this study.

The resulting bicarbonate concentrations were a factor of 2.4 greater on average than the values estimated from gas phase equilibrium considerations. The magnitude of the discrepancy between the two methods of determining bicarbonate concentrations was not dependent on sample pH, but did increase as total inorganic carbon concentration increased in the sample. Overall, the measured inorganic carbon method of determining bicarbonate concentrations yielded a better correlation between anions and cations and did a better job closing the anion/cation deficit than the carbonate estimate that assumes equilibrium with the gas phase (Figure 4). For the subset of samples in which inorganic carbon was measured, the charge balance increased from 0.75 ± 0.13 to 0.91 ± 0.08 when inorganic carbon derived bicarbonate values were used.

3.3 Correlations between radiation fog species

A number of strong, statistically significant ($p<0.01$) correlations were observed between inorganic ions, acetate, formate, TOC, and organic nitrogen (Table 2). These correlations can provide some broad insight into emissions that influence this region. A correlation between sulfate and nitrate ($r = 0.55$) suggests a common source, presumably coal combustion which is the predominant source of sulfur emissions in the US. Chloride was also well correlated with sulfate ($r = 0.63$). This, when coupled with chloride to sodium ratios that were a factor of four greater on average than ratios expected for sea salt, is evidence of a primarily anthropogenic combustion source of chloride rather than a marine source.

Ammonium was strongly correlated with sulfate ($r = 0.92$) and nitrate ($r = 0.69$), reflecting the neutralization of the associated acids either in precursor aerosol particles on which the droplets nucleated or within the fog droplets after their formation. As noted, ammonium was abundant in the fog samples and may have originated to some extent from agricultural fertilizers. If this is the case, correlations might also be expected between the other major macronutrients typically found in

fertilizers, which include phosphate, potassium, and other sources of nitrogen, often in the form of nitrates. Correlations between phosphate and ammonium (r = 0.61), potassium (r = 0.64), and nitrate (r = 0.50), in addition to the aforementioned correlation between ammonium and nitrate, lend some support to the proposition that agricultural fertilizers are one possible source of these species in the fog samples.

Potassium was also found to be well correlated with TOC (r = 0.60). Potassium is often considered to be a marker of biomass combustion, suggesting that some portion of the measured TOC and potassium originated from biomass burning. Local sources of biomass combustion include residential wood-fired boilers, which are common in the area, and at least one nearby industrial facility that burns waste wood and sawdust for process heat.

Acetate and formate were strongly correlated with one another (r = 0.94), indicating a commonality of sources. Unfortunately, the diversity of production pathways that have been identified for those species, including primary biogenic and anthropogenic emissions and secondary production (Chebbi and Carlier, 1996) makes identifying particular sources difficult without additional measurements. Acetate and formate were not strongly correlated with any of the inorganic ions, but they were correlated with TOC, having correlation coefficients of 0.73 (formate) and 0.67 (acetate).

As expected, the crustal derived ions calcium and magnesium were strongly correlated (r = 0.72). Nitrite was most strongly correlated with calcium (r = 0.69) and magnesium (r = 0.53). This suggests that nitrite in the fog samples was not just the result of absorption of gas phase HONO, but was incorporated through scavenging of particulate nitrite as well. The ground surface has been shown to be an important nitrite reservoir as a result of soil-N nitrification/denitrification reactions (Su et al., 2011), deposition of gas phase HONO (VandenBoar et al., 2013), or heterogeneous formation from NO_2 (Acker et al., 2008; 2005). Therefore, the potential exists for crustal materials containing nitrite to be directly lofted into the atmosphere. Alternatively, the emission of gas phase HONO from the surface

may also undergo acid displacement reactions, especially on carbonate containing dust particles (VandenBoar et al., 2014).

Organic nitrogen measured during the study showed correlations with the inorganic nitrogen species ammonium ($r = 0.85$) and nitrate ($r = 0.56$) as well as phosphate ($r = 0.64$). This indicates an agricultural source of organic nitrogen, a finding that has also been noted in precipitation-based organic nitrogen studies (Cape et al., 2011 and reference therein) with further evidence coming from known livestock and fertilizer emissions of individual organic nitrogen species. Other potential sources of organic nitrogen highlighted by Cape et al. (2011) include soil dust and biomass burning. However, the lack of a statistically significant correlations of organic nitrogen with calcium, magnesium, and potassium in this study makes these sources less likely.

3.4 Concentration trends over time

Changes in concentrations over time were evaluated for inorganic ions which were measured over the entire sample collection period. A significant trend was determined to be present if the slope of a linear regression of each ion over time was statistically different than zero ($p<0.01$). To linearize the data, and to satisfy the requirement for normally distributed residuals (Helsel and Hirsch, 2002), the logarithm of the concentration values were used in this analysis. Figure 5 shows these values as a function of time. Significant decreasing trends were observed for sulfate, ammonium, chloride, and pH. Nitrate was also found to decrease over time but at a slightly lower confidence level ($p=0.02$). Also shown in Figure 5 are statistically significant trends in the ratios of nitrate/sulfate and ammonium/(sulfate+nitrate). Potassium, magnesium, and calcium exhibited no significant trends with time. Sodium was below the DL in the majority of samples, so no trend analysis was performed. No significant trends were noted in sample duration over the length of the project. Trends in LWC were difficult to evaluate because LWC data was not available for the entire period, and for the two time

periods when it was available, LWC was determined using different methods as described in Section 2.2. An increasing trend in LWC over the course of the study period could potentially contribute to the observed decreasing trends in ion concentrations as a result of dilution. However, studies that have investigated LWC trends over the last few decades have found that LWC has been decreasing over time in most locations (Klemm and Lin, 2016; Herckes et al., 2015) possibly due to changes in climate or aerosol mass loading. A decreasing trend in LWC, or a lack of a trend in LWC, would suggest that the observed decreases in ion concentrations are the result of changes in emissions rather than dilution.

The trends in sulfate and nitrate likely reflects reductions in emissions that have resulted from enhanced stack-gas scrubbing, improved combustion techniques, and the switch to low sulfur fuels that have been ongoing in the US over the last several decades. Aggregate SO_2 emissions for the US as a whole decreased 52% while SO_2 emissions in the Mid-Atlantic region (US EPA Region 3: Delaware, the District of Columbia, Maryland, Pennsylvania, Virginia, and West Virginia) declined 68% from 2008 through 2014 based on the US EPA's Air Pollutant Emissions Trends Data (US EPA, 2015). This compares to a 76% decrease in sulfate concentrations in the fog samples based on the regression shown in Figure 5. Because fog forms in stagnation conditions and is therefore reflective of local sources, the decommissioning in early 2014 of two local coal combustion sources that lacked SO_2 controls likely played a role in the enhanced decreasing trend in fog sulfate concentration. US emissions of NOx have also declined during the last few decades, but not to the same extent as sulfur. NOx emissions decreased 27% both at the national level and for the Mid-Atlantic region (US EPA, 2015) while fog nitrate concentrations decreased 36% from 2008 to 2014. With concentrations of nitrate decreasing at a slower rate than sulfate in the fog samples, the ratio of nitrate to sulfate increased during the study period. In 2008 the nitrate to sulfate ratio was approximately 0.3 but by 2015 the ratio was approaching an average value of 0.9.

Interestingly, chloride concentrations in the fog samples declined 72% from 2008 through 2014. There are no national inventories for comparison. As noted earlier, the chloride observed in the fog samples does not appear to be associated with sea salt. In the absence of a major sea salt source, the emission of HCl from fossil fuel combustion, primarily coal combustion, was the likely source of chloride in the fog samples (Keene et al., 1999; McCulloch et al., 1999). Along with dedicated HCl removal systems, most of the control technologies employed for SO_2 reductions, including wet and dry scrubbers and the transition away from coal, have the cobenefit of reducing HCl emissions. Therefore, it may not be surprising that the decline in chloride concentrations in the fog samples were similar in magnitude to that noted for suflate.

Ammonium concentrations in the fog samples decreased 35% between 2008 and 2014 even though emissions of ammonia declined only slightly at the national level (3%) and for the Mid-Atlantic region (6%) during that time (US EPA, 2015). Ammonium is incorporated into the fog droplets through scavenging of ammonium containing particles and through the absorption of gas phase ammonia. The observed decline in sulfate and nitrate concentrations in the fog samples suggest that fewer ammonium sulfate and ammonium nitrate particles were being scavenged as time progressed. Furthermore, with fewer acidic inputs in the form of nitric acid or bisulfate to the droplets, droplet pH would tend to be higher, and less ammonium would be absorbed from the gas phase to satisfy partitioning equilibrium. The increase in pH of approximately 1 pH unit over the course of the study supports this argument. As the sum of sulfate and nitrate decreased at a more rapid rate than ammonium, the ratio of ammonium to sulfate plus nitrate more than doubled during the study period, from a value of approximately 1.2 in 2008 to a value of 2.7 in 2015 (Figure 5).

In addition to trends over the length of the study, seasonal trends were also investigated. For a number of species, concentrations tended to be higher in the spring and then decrease as the year progressed. Although there is a great deal of variability, statistically significant ($p<0.01$) decreasing

trends from April through October were observed for nitrate (r = 0.31), ammonium (r = 0.24), potassium (r = 0.27), phosphate (r = 0.37), acetate (r = 0.28), and formate (r = 0.34). Contributing to these decreasing trends may be an increase in LWC from early spring through late fall of approximately 25% ($p<0.02$). However, the trends in concentration are greater than can be accounted for through dilution alone. Instead, these trends may reflect changes in emissions associated with the growing season. Soils have been proposed as a significant source of carboxylic acids to the atmosphere (Talbot et al., 1995) as have direct emissions from vegetation (Chebbi and Carlier, 1996) with both sources exhibiting a seasonal variation that peaks during the growing season. Meanwhile, nitrogen, potassium, and phosphorous are the primary macronutrients in agricultural fertilizers. Emissions from soils and fertilizers may both be enhanced in the spring when soil overturning and fertilizer application are most intense and then decrease in the fall as the growing season comes to a close.

3.5 Comparisons to other radiation fog studies

Inorganic ion concentrations in fog samples collected at the site in central Pennsylvania have been shown to be substantially lower than values measured in fogs and clouds elsewhere in the US (Straub et al., 2012). In terms of radiation fogs, this finding was based on multiple studies in the Central Valley of California, along the US Gulf Coast, and in Indianapolis, IN. The sum of sulfate, nitrate, and ammonium at these locations was typically two to ten times higher, and sometimes 20 to 50 times higher, than the current study. Of the radiation fog studies reviewed, the only site in the US with concentrations similar in magnitude to those measured during the present study was Albany, NY. The relatively higher inorganic ion concentrations reported in the literature extend to international locations as well. For example, the average sum of sulfate, nitrate, and ammonium was eight times greater in the Po Valley in Italy (Giulianelli et al., 2014), four times greater in Poland (Błas et al., 2010), 21 times

greater in Shanghai (Li et al., 2011), eight times greater in Switzerland (Burkard et al., 2003), and 13 times greater in Strasbourg, France (Millet et al., 1996).

While inorganic ion concentrations measured at other locations were much higher than those observed during this study, organic acid concentrations were closer in magnitude to measurements at other locations. This is illustrated in Figure 6, in which formate, acetate, propionate, and oxalate concentrations measured here are compared to those measured in 14 previous radiation fog studies. Because of the disparity between the mean and median values calculated for the current study, both are included in Figure 6. Mean values were most often reported in the literature; however, some only specified median values and are noted as such. When average values are considered, the concentrations of formate and acetate measured in Central Pennsylvania are comparable to some of those found in the Central Valley of California and the Po Valley in Italy, the two regions in which radiation fogs have been the most comprehensively studied. On the other hand, there are a number of studies in which much higher organic acid concentrations were recorded.

The situation is similar for comparisons of TOC concentrations. Herckes et al. (2013) provides a thorough review of organic matter in fogs and clouds and compiles a comprehensive list of fog studies in which TOC or DOC measurements were made. The mean (8.2 mgC l^{-1}) and median (6.6 mgC l^{-1}) values for the present study fall at the lower end of the radiation fog studies reported in Herckes et al. (2013). However, there are several studies in the Central Valley of California and along the US Gulf Coast with values within 20 to 30% of those measured here. Meanwhile, the summary also includes other studies at those locations and elsewhere with TOC or DOC values 2 to 20 times higher than the current study.

3.6 Ammonia Partitioning

The relative abundance of ammonium in the radiation fog samples led to an interest in the abundance of gas phase ammonia in the area and the partitioning of ammonia between the gas and

aqueous phases. Equilibrium considerations imply that measureable amounts of ammonia should have been present in the gas phase during every radiation fog event. As mentioned previously, however, a range of studies have shown that Henry's law equilibrium does not always adequately explain measured partitioning for ammonia or other gases. To investigate the degree to which Henry's law equilibrium was satisfied for ammonia during this study, the measured aqueous phase ammonium concentrations were compared to predicted values based on simultaneously measured gas phase ammonia concentrations.

Gas phase ammonia was measured with an Air Sentry II Ion Mobility Spectrometer (Particle Measuring Systems), an instrument that has been used for the monitoring of ambient ammonia in previous field studies (Myles et al., 2006; Prenni et al., 2014). For this study, calibration was performed with 5 ppm certified ammonia in nitrogen diluted to zero to 50 ppb with a Teledyne API Model 702 precision calibrator. The stated precision for the Air Sentry II is ± 1.5 ppb, and this particular instrument was found to measure ammonia concentrations 0.5 ± 1.1 ppb higher on average than concurrent denuder based ammonia measurements, a conclusion based on an intercomparison of 52 12-hour sample periods (unpublished results).

Ammonia measurements were made between 2012 and 2014. During this period, valid gas phase ammonia concentrations were available for 31 of the radiation fog sample periods. Average ammonia concentrations ranged between 1.5 and 7.8 ppb. For each fog sample period, the average gas phase ammonia concentration was used to calculate a theoretical aqueous phase ammonium concentration according to Henry's law equilibrium. The Henry's law constant for ammonia, dissociation constants for ammonia and water, and temperature dependencies were taken from Seinfeld and Pandis (2006). A ratio of the actual measured ammonium concentration to the theoretical equilibrium ammonium concentration could then be determined for each sample period:

$$R_{aq} = \frac{[NH_4^+]_{aq}}{p_{NH_3} K_H^*} \qquad \text{(Eqn. 3)}$$

Where $[NH_4^+]_{aq}$ is the measured ammonium concentration, p_{NH_3} is the partial pressure of ammonia, and K_H^* is the effective Henry's Law coefficient for ammonia. Values of R_{aq} less than one indicate subsaturation of the aqueous phase and values greater than one indicate supersaturation of the aqueous phase. The values of R_{aq} for the current study are displayed in Figure 7. Although there is a great deal of variability, the ratio of measured to equilibrium concentrations appears to be a function of pH, with supersaturation at higher pH values and subsaturation at lower pH values. Similar trends have been reported for previous studies in which aqueous and gas phase ammonia were simultaneously measured (Figure 7). Voisin et al. (2000) and Sellegri et al. (2003) also found that ammonium was subsaturated by one to two orders of magnitude in supercooled and mixed phase clouds for pH < 5.5.

The trend of increasing subsaturation with decreasing pH, i.e. increasing solubility, suggests that mass transfer limitations may be preventing droplets from attaining equilibrium with the gas phase. Winiwarter et al. (1994) and Ervens et al. (2003) investigated this possibility by developing simple models that specify the aqueous phase concentration as a function of time for droplets having an initial concentration of zero. Both took as their starting points the mass transfer coefficients derived by Schwartz (1986) for gas phase diffusion to a liquid droplet and interfacial transfer across the droplet surface. The combined rate coefficient is given as:

$$k_{mt} = \left[\frac{r^2}{3D_g} + \frac{4r}{3v\alpha}\right]^{-1} \qquad \text{(Eqn. 4)}$$

Where r = droplet radius, D_g = gas phase diffusion coefficient, v = mean molecular speed, and α = accommodation coefficient.

The derivation of Winiwarter et al. (1994) assumes a closed system in which uptake by the droplets reduces the gas phase ammonia concentration. There is no mechanism to slow or stop mass transfer as equilibrium is approached, however, so concentrations greater than equilibrium values cannot be considered realistic. The derivation by Ervens et al. (2003) slows mass transfer to the droplets

as the gradient between gas and aqueous phase decreases and equilibrium is reached. They assume an open system in which gas phase concentrations remain constant.

In either case, the mass transfer limited aqueous phase concentration at a given time can be divided by the aqueous phase concentration assumed to be in equilibrium with the gas phase to produce a ratio similar to R_{aq}. When expressed as a combination of gas phase and interfacial transport, the ratio derived by Winiwarter et al. (1994) can be written as:

$$R_{aq} = \left[exp\left(t - \frac{k_{mt} LWC}{44600 RT}\right) - 1\right] \frac{44600}{LWC\ K_H^*} \quad \text{(Eqn. 5)}$$

Where R = the universal gas constant, T = temperature, LWC = liquid water content, K_H^* is the effective Henry's Law coefficient, k_{mt} is the mass transfer coefficient, and t = time, here considered to be the lifetime of a droplet. The ratio based on the derivation of Ervens et al. (2003) can be expressed as:

$$R_{aq} = -exp\left(-t \frac{k_{mt}}{K_H^*\, RT}\right) + 1 \quad \text{(Eqn. 6)}$$

Where the variable definitions are the same as for Equation 5. These ratios are shown in Figure 7 as a function of pH for conditions that represent a realistic upper limit on mass transfer limitations (LWC = 0.25 g m^{-3}, r = 10 µm, t = 60 s, T = 273 K, and α = 0.001), along with values for Dg = 0.1 cm^2 s^{-1} and v = 5800 cm s^{-1} (Winiwarter et al., 1994). For these conditions, there is good agreement between the two approaches. To illustrate the sensitivity to droplet lifetime, temperature, and accommodation coefficient, ratios for different values of those parameters are also shown in Figure 7. For a longer droplet lifetime, an increase in temperature, or a larger accommodation coefficient, limitations on mass transfer are less severe and the degree of subsaturation decreases. Overall, the trend with pH for any of the sets of conditions is similar to those obtained from measured concentrations, both for the current study and for previous studies, indicating that mass transport limitations play a significant role in the adjustment of the aqueous phase to equilibrium.

Although these models only treat transfer from the gas phase to the aqueous phase, the reverse could also be a plausible explanation for the observations of supersaturated conditions. As fog droplets form on ammonium containing particles, the result may be aqueous concentrations that exceed equilibrium values. In this case, mass transport limitations could prevent the droplets from rapidly outgassing and reaching equilibrium over the lifetime of the droplets. Alternatively, supersaturation of the aqueous phase could also result from the collection of a bulk samples from a population of droplets that vary in pH. Pandis and Seinfeld (1991) have shown that the mixing of droplets that are individually in equilibrium with the gas phase may result in a bulk sample that is no longer in equilibrium, and can result in R_{aq} values up to 3. Ervens et al. (2003) found more modest results for this effect, with R_{aq} ranging between 1.12 and 1.48 for variations of 1 pH unit across a measured drop size distribution.

4. Conclusions

The chemical composition of radiation fog has been documented over a period of 8 years at a rural location in Central Pennsylvania, revealing long term and seasonal trends, offering insight into emission sources in the region, and providing an indication of local air quality. During those eight years, 146 samples were collected with an automated CHRCC and then analyzed for pH, inorganic ions, organic acids, TOC, and TN. Concentrations and pH values varied widely from sample to sample. For example, the median ammonium concentration was 209 μN with a range between 31 μN and 1277 μN. Ammonium, sulfate, calcium, and nitrate were the most abundant inorganic ions measured while acetate and formate dominated organic acid concentrations. Organic acids accounted for 15% of TOC on average leaving the majority of TOC unspeciated in this study. TN was dominated by inorganic nitrogen species, with 18% being attributed to organic nitrogen. While this fraction of organic nitrogen is similar to previous studies, the absolute concentrations of organic nitrogen measured during this study were much lower than previous studies. The median pH was 6.46, but varied between 3.08 and

7.41. Organic acids contributed significantly to the acidification of the lowest pH samples, while neutralization primarily by ammonium resulted in samples with high pH.

The inorganic ion concentrations measured during this study were much lower than for radiation fogs sampled at other sites where measured values were at least a factor of two higher, and often much higher than that. Given that radiation fogs form under stagnation conditions and are efficient scavengers of particles and soluble gases, they are representative of the overall loading of pollutants in the local area. The lower inorganic loadings observed during this study are likely the result of the sampling site's rural setting and associated lack of urban or major industrial emission sources. On the other hand, concentrations of organic acids and TOC were in closer agreement with studies conducted elsewhere, perhaps as a result of farming related emissions in this predominantly agricultural region. With comparatively lower inorganic concentrations, and more typical TOC concentrations, the contribution of organic matter to total solute mass in the fog samples collected at the study site was found to be higher than at other locations. Organic matter contributed 52% on average to the total solute mass during this study compared to values of 33% or less in the Central Valley of California, the Po Valley in Italy, and along the US Gulf Coast.

Based on correlations between species and concentration trends over time, the main emission sources that influence this region could be broadly categorized. Anthropogenic combustion was identified through statistically significant correlations between sulfate, nitrate, and chloride. Long term decreasing trends were also noted for each of these ions, with sulfate declining the most (76%) followed by chloride (72%) and nitrate (36%) for the period 2008 - 2014. These trends were consistent with documented reductions in US emissions, which come primarily from power generation facilities. Due to the steeper decline in sulfate, the ratio of nitrate to sulfate rose during this period from 0.3 to 0.9. Correlations between ions that comprise the major macronutrients in fertilizer, i.e. phosphate, potassium, nitrate, and ammonium, indicate that emissions from agricultural fertilizers impacted this

region. Decreasing trends in these ions as the growing season progressed lends support to this conclusion. Because potassium is considered to be a tracer for biomass burning, its presence in the fog samples and its strong correlation with TOC indicate that biomass combustion is a source of emissions in the local area. Finally, correlations between calcium, magnesium, and nitrite provide evidence of a crustal emission source.

The practice of using gas phase CO_2 concentrations and Henry's law equilibrium to determine aqueous bicarbonate concentrations appears to underestimate the actual amount of bicarbonate present in samples collected during this study. This conclusion was based on measurements of inorganic carbon that were available for a subset of the fog water samples. When bicarbonate concentrations derived from measured inorganic carbon were used in place of those based on CO_2 equilibrium, the correlation between anions and cations improved and the ion balance was closer to unity. The apparent lack of equilibrium between the gas and aqueous phases was also observed for ammonium during sample periods in which gas phase ammonia was concurrently measured. Aqueous phase ammonium concentrations were lower than equilibrium predictions for low pH samples and higher than predictions for high pH samples. For subsaturated samples in this and previous studies, the trend in subsaturation as a function of pH suggests that the transfer of gas phase ammonia into the liquid droplets is limited by gas phase diffusion and interfacial transport. Supersaturated samples may be the result of the bulk collection process in which droplets of varying size and pH are individually in equilibrium with the gas phase but do not remain in equilibrium once mixed. Although not explicitly addressed here, nucleation scavenging of ammonium containing particles coupled with limitations on mass transfer out of the droplets could also result in supersaturation.

5. Acknowledgements

The author gratefully acknowledges the valuable contributions of Dan Ressler who performed the TOC and TN analyses and Pierre Herckes and James Hutchings who assisted with sample analysis early in the project. Susquehanna University is also deserving of acknowledgment for supporting this work over the duration of the study.

6. References

Acker K., Beysens D., Möller D., 2008. Nitrite in dew, fog, cloud and rain water: An indicator for heterogeneous processes on surfaces. *Atmospheric Research*, *87*(3), 200-212.

Acker K., Möller D., Auel R., Wieprecht W., Kalass, D., 2005. Concentrations of nitrous acid, nitric acid, nitrite and nitrate in the gas and aerosol phase at a site in the emission zone during ESCOMPTE 2001 experiment. *Atmospheric Research*, *74*(1), 507-524.

Acker K., Möller D., Wieprecht W., 1995. Mt. Brocken, a site for a cloud chemistry measurement programme in Central Europe. *Water, Air, and Soil Pollution*, *85*(4), 1979-1984.

Aikawa M., Hiraki T., Shoga M., Tamaki M., Sumitomo S., 2007. Seven-year trend and the time and seasonal dependence of fog water collected near an industrialized area in Japan. *Atmospheric Research*, *83*(1), 1-9.

Aleksic N., Roya K., Sistla G., Dukett J., Houck N., Casson P., 2009. Analysis of cloud and precipitation chemistry at Whiteface Mountain, NY. *Atmospheric Environment*, 43, 2709–2716.

Anderson J.B., Baumgardner R.E., Grenville S.E., 2006. Trends in cloud water sulfate and nitrate as measured at two mountain sites in the Eastern United States: Regional contributions and temporal changes compared with regional changes in emissions, 1986–1999. *Atmospheric Environment*, *40*(23), 4423-4437.

Anderson J.B., Baumgardner R.E., Mohnen V.A., Bowser J.J., 1999. Cloud chemistry in the Eastern United States, as sampled from three high-elevation sites along the Appalachian Mountains. *Atmospheric Environment*, 33, 5105-5114.

Baumgardner Jr. R.E., Isil S.S., Lavery T.F., Rogers C.M., & Mohnen V.A., 2003. Estimates of cloud water deposition at mountain acid deposition program sites in the Appalachian Mountains. *Journal of the Air & Waste Management Association*, *53*(3), 291-308.

Błaś M., Polkowska Ż., Sobik M., Klimaszewska K., Nowiński K., Namieśnik J., 2010. Fog water chemical composition in different geographic regions of Poland. *Atmospheric Research*, *95*(4), 455-469.

Burkard R., Butzberger P., Eugster W., 2003. Vertical fogwater flux measurements above an elevated forest canopy at the Lageren research site, Switzerland. *Atmospheric Environment,* 37, 2979-2990.

Cape J.N., Cornell S.E., Jickells T.D., Nemitz E., 2011. Organic nitrogen in the atmosphere—Where does it come from? A review of sources and methods. *Atmospheric Research*, *102*(1), 30-48.

Capel P.D., Gunde R., Zuercher F., Giger W., 1990. Carbon speciation and surface tension of fog. *Environmental Science and Technology,* 24, 722-727.

Carrillo J.H., Emert S.E., Sherman D.E., Herckes P., Collett Jr. J.L., 2008. An economical optical cloud/fog detector. *Atmospheric Research*, 87, 259-267.

Chebbi A., Carlier P., 1996. Carboxylic acids in the troposphere, occurrence, sources, and sinks: A review. *Atmospheric Environment*, *30*(24), 4233-4249.

Collett Jr. J.L., Herckes P., Youngster S., Lee T., 2008. Processing of atmospheric organic matter by California radiation fogs. *Atmospheric Research*, 87, 232-241.

Collett Jr. J.L., Sherman D.E., Moore K.F., Hannigan M.P., and Lee T., 2001. Aerosol particle processing and removal by fogs: observations in chemically heterogeneous central California radiation fogs. *Water, Air and Soil Pollution: Focus*, *1*(5-6), 303-312.

Collett Jr. J.L., Hoag J.K., Sherman D.E., Bator A., Richards L.W., 1999. Spatial and temporal variations in San Joaquin Valley fog chemistry. *Atmospheric Environment*, 33, 129-140.

Dall'Osto M., Harrison R.M., Coe H., Williams P., 2009. Real-time secondary aerosol formation during a fog event in London. *Atmospheric Chemistry and Physics*, *9*(7), 2459-2469.

Degefie D.T., El-Madany T.-S., Hejkal J., Held M., Dupont J.C., Haeffelin M., Klemm O., 2015. Microphysics and energy and water fluxes of various fog types at SIRTA, France. *Atmospheric Research*, 151, 162-175.

Deguillaume L., Charbouillot T., Joly M., Vaitilingom M., Parazols M., Marinoni A., Amato P., Delort A.M., Vinatier V., Flossmann A., Chaumerliac N., Pichon J.M., Houdier S., Laj P., Sellegri K., Colomb A., Brigante M., Mailhot G., 2014. Classification of clouds sampled at the puy de Dôme (France) based on 10 yr of monitoring of their physicochemical properties. *Atmospheric Chemistry and Physics*, *14*, 1485-1506.

Demoz B.B., Collett Jr. J.L., Daube Jr. B.C., 1996. On the Caltech active strand cloudwater collectors. *Atmospheric Research*, 41, 47-62.

Ehrenhauser F. S., Khadapkar K., Wang Y., Hutchings J.W., Delhomme O., Kommalapati R. R., Herckes P., Wornat M.J., Valsaraj K.T., 2012. Processing of atmospheric polycyclic aromatic hydrocarbons by fog in an urban environment. *Journal of Environmental Monitoring*, *14*(10), 2566-2579.

Ervens B., Wang Y., Eagar J., Leaitch W.R., Macdonald A.M., Valsaraj K.T., Herckes P., 2013. Dissolved organic carbon (DOC) and select aldehydes in cloud and fog water: the role of the aqueous phase in impacting trace gas budgets. *Atmospheric Chemistry and Physics*, *13*(10), 5117-5135.

Ervens B., Herckes P., Feingold G., Lee T., Collett J.L., Kreidenweis, S.M., 2003. On the drop-size dependence of organic acid and formaldehyde concentrations in fog. *Journal of Atmospheric Chemistry*, 46, 239-269.

Facchini M.C., Fuzzi S., Zappoli S., Andracchio A., Gelencsér A., Kiss G., Krivacsy Z., Meszaros E., Hansson H.-C., Alsberg T., Zebühr Y., 1999. Partitioning of the organic aerosol component between fog droplets and interstitial air. *Journal of Geophysical Research: Atmospheres*, *104*(D21), 26821-26832.

Facchini M.C., Fuzzi S., Kessel M., Wobrock W., Jaeschke W., Arends B.G., Mols, J.J., Berner A., Solly I., Kruisz C., Reischl, G., Pahl S., Hallberg A., Ogren J.A., Fierlinger-Oberlinninger H., Marzorati A., Schell D., 1992a. The chemistry of sulfur and nitrogen species in a fog system A multiphase approach. *Tellus B*, *44*(5), 505-521.

Facchini M.C., Fuzzi S., Lind J.A., Fierlinger-Oberlinninger H., Kalina M., Puxbaum H., Winiwarter W., Arends B.G., Wobrock W., Jaeschke W., Berner A., Kruisz C., 1992b. Phase-partitioning and chemical reactions of low molecular weight organic compounds in fog. *Tellus B*, *44*(5), 533-544.

Fahey K.M., Pandis S.N., Collett J.L., Herckes P., 2005. The influence of size-dependent droplet composition on pollutant processing by fogs. *Atmospheric Environment*, *39*(25), 4561-4574.

Fuzzi S., Facchini M.C., Decesari S., Matta E., Mircea M., 2002. Soluble organic compounds in fog and cloud droplets: what have we learned over the past few years? *Atmospheric Research*, *64*(1), 89-98.

George J.J., 1951. Fog. In *Compendium of Meteorology*, T. F. Malone, Ed., American Meteorological Society, 1179–1189.

Gilardoni S., Massoli P., Giulianelli L., Rinaldi M., Paglione M., Pollini F., Lanconelli C., Poluzzi V., Carbone S., Hillamo R., Russell, L.M., Facchini M.C., Fuzzi S., 2014. Fog scavenging of organic and inorganic aerosol in the Po Valley. *Atmospheric Chemistry and Physics*, *14*(13), 6967-6981.

Gioda A., Mayol-Bracero O.L., Scatena F.N., Weathers K.C., Mateus V.L., McDowell W.H., 2013. Chemical constituents in clouds and rainwater in the Puerto Rican rainforest: potential sources and seasonal drivers. *Atmospheric Environment*, *68*, 208-220.

Giulianelli L., Gilardoni S., Tarozzi L., Rinaldi M., Decesari S., Carbone C., Facchini M.C., Fuzzi S., 2014. Fog occurrence and chemical composition in the Po valley over the last twenty years. *Atmospheric Environment*, *98*, 394-401.

Gultepe I., Tardif R., Michaelides S.C., Cermak J., Bott A., Bendix J., Müller M.D., Pagowski M., Hansen B., Ellrod G., Jacobs W., Toth G., Cober S.G., 2007. Fog research: A review of past achievements and future perspectives. *Pure and Applied Geophysics*, 164, 1121-1159.

Helsel D.R., Hirsch R.M., 2002. *Statistical Methods in Water Resources*, Techniques of Water Resources Investigations, Book 4, chapter A3. U.S. Geological Survey. 522 pages.

Herckes P., Marcotte A.R., Wang Y., Collett J.L., 2015. Fog composition in the Central Valley of California over three decades. *Atmospheric Research*, *151*, 20-30.

Herckes P., Valsaraj K.T., Collett J.L., 2013. A review of observations of organic matter in fogs and clouds: Origin, processing and fate. *Atmospheric Research*, *132*, 434-449.

Herckes P., Chang H., Lee T., Collett Jr. J.L., 2007. Air pollution processing by radiation fogs. *Water, Air, and Soil Pollution*, 181, 65-75.

Herckes P., Wortham H., Mirabel P., Millet M., 2002a. Evolution of the fogwater composition in Strasbourg (France) from 1990 to 1999. *Atmospheric Research*, 64, 53-62.

Herckes P., Lee T., Trenary L., Kang G., Chang H., Collett Jr. J.L., 2002b. Organic matter in Central California radiation fogs. *Environmental Science and Technology*, 36, 4777-4782.

Herckes P., Hannigan M.P., Trenary L., Lee T., Collett Jr. J.L., 2002c. Organic compounds in radiation fogs in Davis (California). *Atmospheric Research*, 64, 99-108.

Jacob D.J., Munger J.W., Waldman J.M., Hoffmann M.R., 1986. The H_2SO_4-HNO_3-NH_3 system at high humidities and in fogs 1. Spatial and temporal patterns in the San Joaquin Valley of California. *Journal of Geophysical Research*, 91, 1073–1088.

Jaeschke W., Dierssen J.P., Günther A., Schumann M., 1998. Phase partitioning of ammonia and ammonium in a multiphase system studied using a new vertical wet denuder technique. *Atmospheric Environment*, *32*(3), 365-371.

Kaul D.S., Gupta T., Tripathi S.N., Tare V., Collett J.L., 2011. Secondary organic aerosol: a comparison between foggy and nonfoggy days. *Environmental science & technology*, *45*(17), 7307-7313.

Keene W.C., Khalil M.A.K., Erickson D.J., McCulloch A., Graedel T.E., Lobert J.M., Aucott M.L., Gong S.L., Harper D.B., Kleiman G., Midgley, P., Moore R.M., Seuzaret C., Sturges W.T., Benkovitz C.M., Koropalov V., Barrie L.A., Li Y.F., 1999. Composite global emissions of reactive chlorine from

anthropogenic and natural sources: Reactive Chlorine Emissions Inventory. *Journal of Geophysical Research: Atmospheres*, *104*(D7), 8429-8440.

Khemani L.T., Momin G.A., Rao P.S.P., Safai P.D., Prem, P., 1987. Influence of alkaline particulates on the chemistry of fog water at Delhi, North India. *Water, Air and Soil Pollution*, 34, 183–189.

Klemm O., Lin N.-H., 2016. What Causes Observed Fog Trends: Air Quality or Climate Change? *Aerosol and Air Quality Research*, 16, 1131–1142.

Laj P., Fuzzi S., Facchini M.C., Lind J.A., Orsi G., Preiss M., Maser R., Jaeschke W., Seyffer E., Helas G., Acker K., Wieprecht W., Moller D., Arends B.G., Mols J.J., Colvile R.N., Gallagher M.W., Beswick K.M., Hargreaves K.J., Storeton-West R.L., Sutton M.A., 1997. Cloud processing of soluble gases. *Atmospheric Environment*, *31*(16), 2589-2598.

Lakhani A., Parmar R.S., Satsangi G.S., Prakash, S., 2007. Chemistry of fogs at Agra, India: Influence of soil particulates and atmospheric gases. *Environmental Monitoring and Assessment*, 133(1-3), 435-445.

Li P., Li X., Yang C., Wang X., Chen J., Collett J.L., 2011. Fog water chemistry in Shanghai. *Atmospheric Environment*, *45*(24), 4034-4041.

Liu D., Yang J., Niu S., Li Z., 2011. On the evolution and structure of a radiation fog event in Nanjing. *Advances in Atmospheric Sciences*, *28*, 223-237.

McCulloch A., Aucott M.L., Benkovitz C.M., Graedel T.E., Kleiman G., Midgley P.M., Li, Y.F., 1999. Global emissions of hydrogen chloride and chloromethane from coal combustion, incineration and industrial activities: Reactive Chlorine Emissions Inventory. *Journal of Geophysical Research: Atmospheres*, *104*(D7), 8391-8403.

McGregor K.G., Anastasio C., 2001. Chemistry of fog waters in California's Central Valley: 2. Photochemical transformations of amino acids and alkyl amines. *Atmospheric Environment*, *35*(6), 1091-1104.

Millet M., Wortham H., Sanusi A., Mirabel P., 1997. Low molecular weight organic acids in fogwater in an urban area: Strasbourg (France). *Science of the Total Environment,* 206, 57-65.

Millet M., Sanusi A., Wortham H., 1996. Chemical composition of fogwater in an urban area: Strasbourg (France). *Environmental Pollution*, 94, 345-354.

Mohnen V.A., Kadlecek J.A., 1989. Cloud chemistry research at Whiteface Mountain. *Tellus B,* 41B, 79–91.

Moore K.F., Sherman D.E., Reilly J.E., Collett J.L., 2004a. Drop size-dependent chemical composition in clouds and fogs. Part I. Observations. *Atmospheric Environment*, *38*(10), 1389-1402.

Moore K.F., Sherman D.E., Reilly J.E., Hannigan M.P., Lee T., Collett J.L., 2004b. Drop size-dependent chemical composition of clouds and fogs. Part II: Relevance to interpreting the aerosol/trace gas/fog system. *Atmospheric Environment*, *38*(10), 1403-1415.

Munger J.W., Collett J.L., Daube B.C., Hoffmann, M.R., 1989. Carboxylic acids and carbonyl compounds in southern California clouds and fogs. *Tellus B*, *41*(3), 230-242.

Murray G.L., Kimball K.D., Hill L.B., Hislop J.E., Weathers K.C., 2013. Long-term trends in cloud and rain chemistry on Mount Washington, New Hampshire. *Water, Air, & Soil Pollution*, *224*(9), 1-14.

Myles L., Meyers T.P., Robinson L., 2006. Atmospheric ammonia measurement with an ion mobility spectrometer. *Atmospheric Environment*, *40*(30), 5745-5752.

National Oceanic and Atmospheric Administration, 2002. The Climate Atlas of the United States, Version 2.0. National Climatic Data Center, Asheville, N.C.

Pandis S.N., Seinfeld J.H., 1991. Should bulk cloudwater or fogwater samples obey Henry's law? *Journal of Geophysical Research: Atmospheres*, *96*(D6), 10791-10798.

Prenni A.J., Levin E.J.T., Benedict K.B., Sullivan A.P., Schurman M.I., Gebhart K.A., Day D.E., Carrico C.M., Malm W.C., Schichtel B.A., Collett Jr. J.L., Kreidenweis S.M., 2014. Gas-phase reactive nitrogen near Grand Teton National Park: Impacts of transport, anthropogenic emissions, and biomass burning. *Atmospheric Environment*, *89*, 749-756.

Raja S., Raghunathan R., Kommalapati R.R., Shen X., Collett Jr. J.L., Valsaraj K.T., 2009. Organic composition of fogwater in the Texas-Louisiana Gulf Coast corridor. *Atmospheric Environment*, 43, 4214-4222.

Raja S., Raghunathan R., Yu X.-Y., Lee T., Chen J., Kommalapati R.R., Murugesan K., Shen X., Qingzhong Y., Valsaraj K.T., Collett Jr. J.L., 2008. Fog chemistry in the Texas-Louisiana Gulf Coast corridor. *Atmospheric Environment*, 42, 2048-2061.

Raja S., Ravikrishna R., Kommalapati R., Valsaraj K., 2005. Monitoring of fogwater chemistry in the Gulf Coast urban industrial corridor: Baton Rouge (Louisiana). *Environmental Monitoring and Assessment,* 110, 99-110.

Reilly J.E., Rattigan O.V., Moore K.F., Judd C., Sherman D.E., Dutkiewicz V.A., Kreidenweis S.M., Husain L., Collett Jr. J.L., 2001. Drop size-dependent S(IV) oxidation in chemically heterogeneous radiation fogs. *Atmospheric Environment,* 35, 5717-5728.

Schemenauer R.S., Banic C.M., Urquizo N., 1995. High elevation fog and precipitation chemistry in southern Quebec, Canada. *Atmospheric Environment,* 29, 2235-2252.

Schwartz, S., 1986: Mass transport considerations pertinent to aqueous phase reactions of gases in liquid water clouds, in Jaeschke, W. (ed.), Chemistry of Multiphase Atmospheric Systems, NATO ASI Series, Springer, Berlin, pp. 415–471.

Seinfeld, J.H., Pandis, S.N., 2006. *Atmospheric chemistry and physics: from air pollution to climate change*. 2nd Ed., Wiley-Interscience, New York, NY, 1232pp.

Sellegri K., Laj P., Marinoni A., Dupuy R., Legrand M., Preunkert S., 2003. Contribution of gaseous and particulate species to droplet solute composition at the Puy de Dôme, France. *Atmospheric Chemistry and Physics*, *3*(5), 1509-1522.

Straub D.J., Hutchings J.W., Herckes P., 2012. Measurements of fog composition at a rural site. *Atmospheric Environment*, *47*, 195-205.

Su H., Cheng Y., Oswald R., Behrendt T., Trebs I., Meixner F.X., Andreae M.O., Cheng P., Zhang Y., Pöschl, U., 2011. Soil nitrite as a source of atmospheric HONO and OH radicals. *Science*, *333*(6049), 1616-1618.

Tago H., Kimura H., Kozawa K., Fujie K., 2006. Long-term observation of fogwater composition at two mountainous sites in Gunma Prefecture, Japan. *Water, Air, and Soil Pollution*, *175*(1-4), 375-391.

Talbot R.W., Mosher B.W., Heikes B.G., Jacob D.J., Munger J.W., Daube B.C., Keene W.C., Maben J.R., Artz R.S., 1995. Carboxylic acids in the rural continental atmosphere over the eastern United States during the Shenandoah Cloud and Photochemistry Experiment. *Journal of Geophysical Research: Atmospheres*, *100*(D5), 9335-9343.

U.S. Environmental Protection Agency, 2015. Air Pollutant Emissions Trends Data. Available online at https://www.epa.gov/air-emissions-inventories/air-pollutant-emissions-trends-data.

Vaïtilingom M., Attard E., Gaiani N., Sancelme M., Deguillaume L., Flossmann A. I., Amato P., Delort, A.-M., 2012. Long-term features of cloud microbiology at the puy de Dôme (France). *Atmospheric Environment*, *56*, 88-100.

VandenBoer T.C., Markovic M.Z., Sanders J.E., Ren X., Pusede S.E., Browne E.C., Cohen R.C., Zhang L., Thomas J., Brune W.H., Murphy J.G., 2014. Evidence for a nitrous acid (HONO) reservoir at the ground surface in Bakersfield, CA, during CalNex 2010. *Journal of Geophysical Research: Atmospheres*, *119*(14), 9093-9106.

VandenBoer T.C., Brown S.S., Murphy J.G., Keene W.C., Young C.J., Pszenny A.A.P., Kim S., Warneke C., de Gouw J.A., Maben J.R., Wagner N.L., Riedel T.P., Thornton J.A., Wolfe D.E. Dube W.P., Ozturk F., Brock C.A., Grossberg N., Lefer B., Lerner B., Middlebrook A.M., Roberts J.M., 2013. Understanding the role of the ground surface in HONO vertical structure: High resolution vertical profiles during NACHTT-11. *Journal of Geophysical Research: Atmospheres*, *118*(17), doi:10.1002/2013JD020971.

Voisin D., Legrand M., Chaumerliac N., 2000. Scavenging of acidic gases (HCOOH, CH_3COOH, HNO_3, HCl, and SO_2) and ammonia in mixed liquid-solid water clouds. *Journal of Geophysical Research*, *105*(D5), 6817-6835.

Wang Y., Zhang J., Marcotte A.R., Karl M., Dye C., Herckes P., 2015. Fog chemistry at three sites in Norway. *Atmospheric Research*, *151*, 72-81.

Winiwarter W., Fierlinger H., Puxbaum H., Facchini M.C., Arends B.G., Fuzzi S., Schell D., Kaminski U., Pahl S., Schneider T., Berner A., Solly I., Kruisz C., 1994. Henry's law and the behavior of weak acids and bases in fog and cloud. *Journal of Atmospheric Chemistry*, *19*(1-2), 173-188.

Winiwarter W., Brantner B., Puxbaum H., 1992. Comment on “Should bulk cloudwater or fogwater samples obey Henry's law?” by SN Pandis and JH Seinfeld. *Journal of Geophysical Research: Atmospheres*, *97*(D5), 6075-6078.

Winiwarter W., Puxbaum H., Fuzzi S., Facchini M.C., Orsi G., Beltz N., Enderle K., Jaeschke W., 1988. Organic acid gas and liquid-phase measurements in Po Valley fall-winter conditions in the presence of fog. *Tellus B*, 40B, 348-357.

Yamaguchi T., Katata G., Noguchi I., Sakai S., Watanabe Y., Uematsu M., Furutani H., 2015. Long-term observation of fog chemistry and estimation of fog water and nitrogen input via fog water deposition at a mountainous site in Hokkaido, Japan. *Atmospheric Research*, *151*, 82-92.

Zhang Q., Anastasio C., 2003a. Conversion of fogwater and aerosol organic nitrogen to ammonium, nitrate, and NOx during exposure to simulated sunlight and ozone. *Environmental Science and Technology*, 37, 3522-3530.

Zhang Q., Anastasio C., 2003b. Free and combined amino compounds in atmospheric fine particles (PM2.5) and fog waters from Northern California. *Atmospheric Environment*, 37, 2247-2258.

Zhang Q., Anastasio C., 2001. Chemistry of fog waters in California's Central Valley--Part 3: concentrations and speciation of organic and inorganic nitrogen. *Atmospheric Environment*, 35, 5629-5643.

	Units	DL	RSD	No. of Samples	Average	Median	Min	Max
pH	-	-	-	146	4.65[a]	6.46	3.08	7.41
Na^+	µN	7.9	3.2%	134	5.7	3.9	< DL	53.8
NH_4^+	µN	6.0	2.3%	134	244.0	209.0	31.2	1277.4
K^+	µN	1.1	3.0%	134	8.9	6.5	< DL	93.1
Mg^{2+}	µN	1.8	3.9%	134	6.2	4.9	< DL	23.1
Ca^{2+}	µN	5.1	2.3%	134	71.0	50.5	5.1	402.6
Cl^-	µN	1.3	4.3%	134	14.9	9.4	2.5	103.9
NO_2^-	µN	0.8	3.0%	97	11.5	9.2	1.2	66.0
NO_3^-	µN	0.4	3.3%	134	48.1	31.4	4.5	398.3
SO_4^{2-}	µN	1.0	2.7%	134	105.1	69.2	7.3	955.4
F^-	µN	0.2	4.9%	94	1.6	0.8	<DL	26.0
PO_4^{3-}	µN	0.7	3.1%	94	7.6	5.1	1.3	70.1
[b]HCO_3^-	µN	-	-	146	28.5	21.9	0.0	242.8
[c]Acetate	µM	1.3	3.4%	94	40.2	21.2	1.7	696.6
[c]Formate	µM	1.4	4.0%	94	53.3	19.6	3.2	1182.1
TOC	mgC L^{-1}	0.3	5.0%	67	8.2	6.6	2.2	28.1
TN	mgN L^{-1}	0.3	5.1%	55	4.1	3.6	1.6	11.5

[a] based on average H^+ concentration

[b] calculated based on assumption of equilibrium with gas phase CO_2

[c] represents ionic plus non-ionic forms

Table 1. Detection limits (DL) at the 95% confidence limit and relative standard deviations (RSD) for the fog water analyses and statistical summary of sample composition.

	Cl^-	NO_3^-	SO_4^{2-}	NO_2^-	PO_4^{3-}	Ac^-	For^-	Na^+	NH_4^+	K^+	Mg^{2+}	Ca^{2+}	*TOC*	*ON*
Cl^-	1.00													
NO_3^-	**0.30**	1.00												
SO_4^{2-}	**0.63**	**0.55**	1.00											
NO_2^-	0.05	-0.06	-0.02	1.00										
PO_4^{3-}	**0.33**	**0.50**	**0.41**	0.03	1.00									
Ac^-	0.22	0.05	0.03	0.15	0.14	1.00								
For^-	0.26	0.13	0.10	0.02	**0.27**	**0.94**	1.00							
Na^+	**0.47**	0.08	0.10	0.17	0.24	0.02	0.02	1.00						
NH_4^+	**0.52**	**0.69**	**0.92**	0.17	**0.61**	-0.01	0.04	0.10	1.00					
K^+	**0.23**	0.15	0.18	0.24	**0.64**	0.12	0.20	0.05	0.19	1.00				
Mg^{2+}	**0.36**	0.20	**0.28**	**0.53**	**0.27**	**0.38**	**0.30**	0.13	**0.25**	**0.33**	1.00			
Ca^{2+}	**0.27**	0.02	0.20	**0.69**	0.14	0.21	0.12	0.17	0.15	0.15	**0.72**	1.00		
TOC	**0.39**	**0.36**	0.25	**0.31**	**0.41**	**0.73**	**0.67**	0.00	**0.49**	**0.60**	**0.45**	0.31	1.00	
ON	0.28	**0.56**	**0.72**	0.04	**0.64**	-0.03	-0.12	0.15	**0.85**	0.25	0.05	-0.05	**0.39**	1.00

Table 2. Correlation coefficients for inorganic ions, acetate, formate, TOC, and organic nitrogen measured in the fog samples. Bold values indicate statistical significance ($p<0.01$).

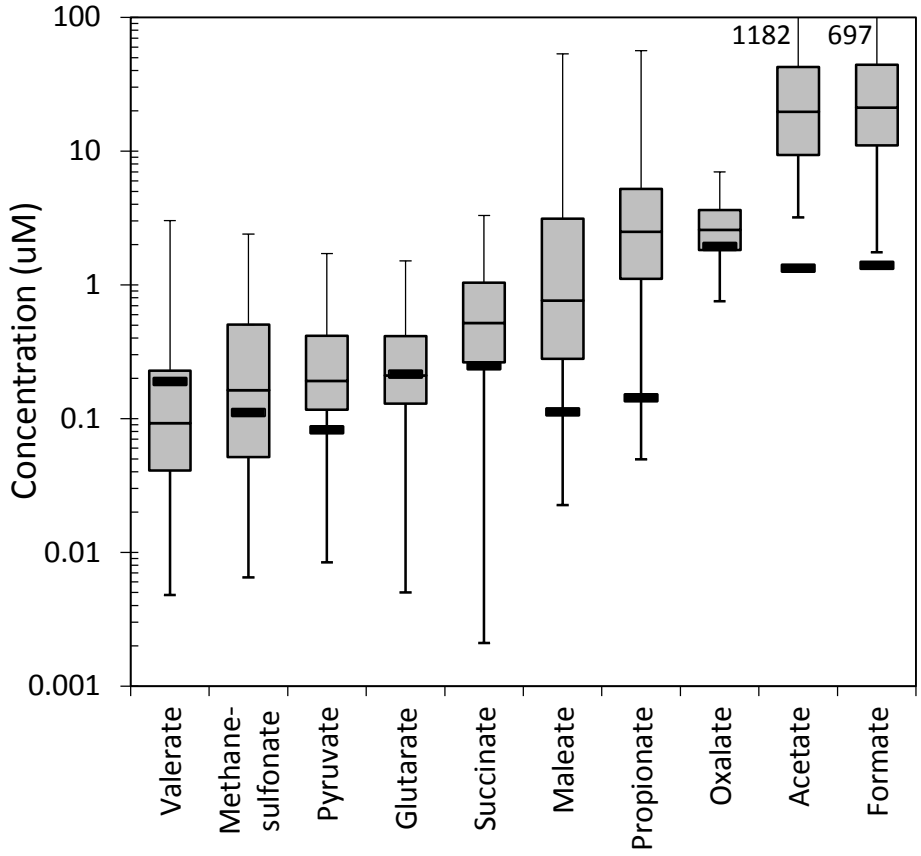

Figure 1. Concentrations of low molecular weight organic acids measured in 94 samples collected between 2012 and 2015. The central solid line represents the median, the box represents the 25th and 75th percentiles, and the error bars represent the minimum and maximum values of the measurements. The thick horizontal lines represent detection limits.

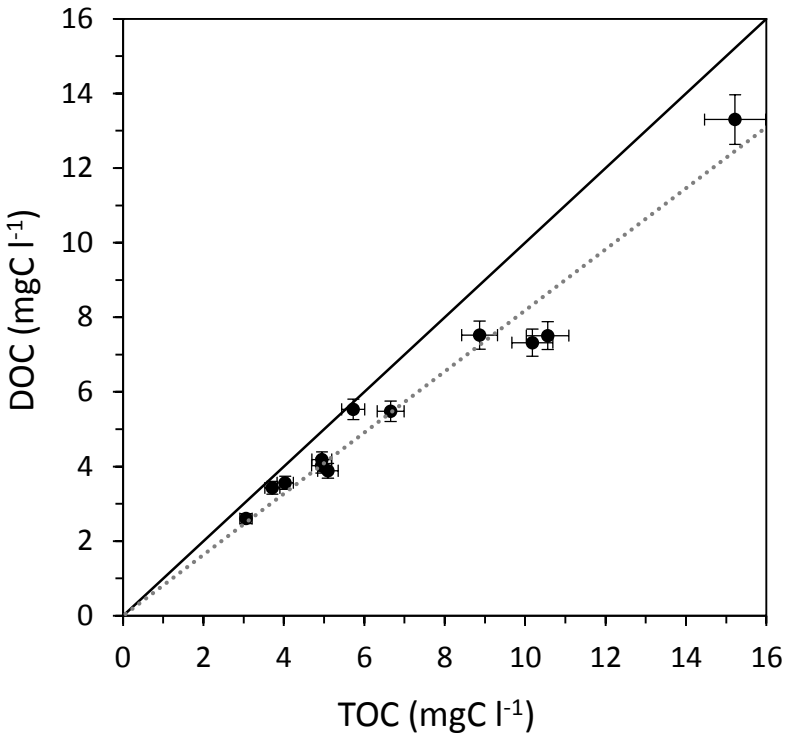

Figure 2. Concentrations of DOC vs. TOC for 12 samples collected in 2014 and 2015. Error bars represent 5% RSD.

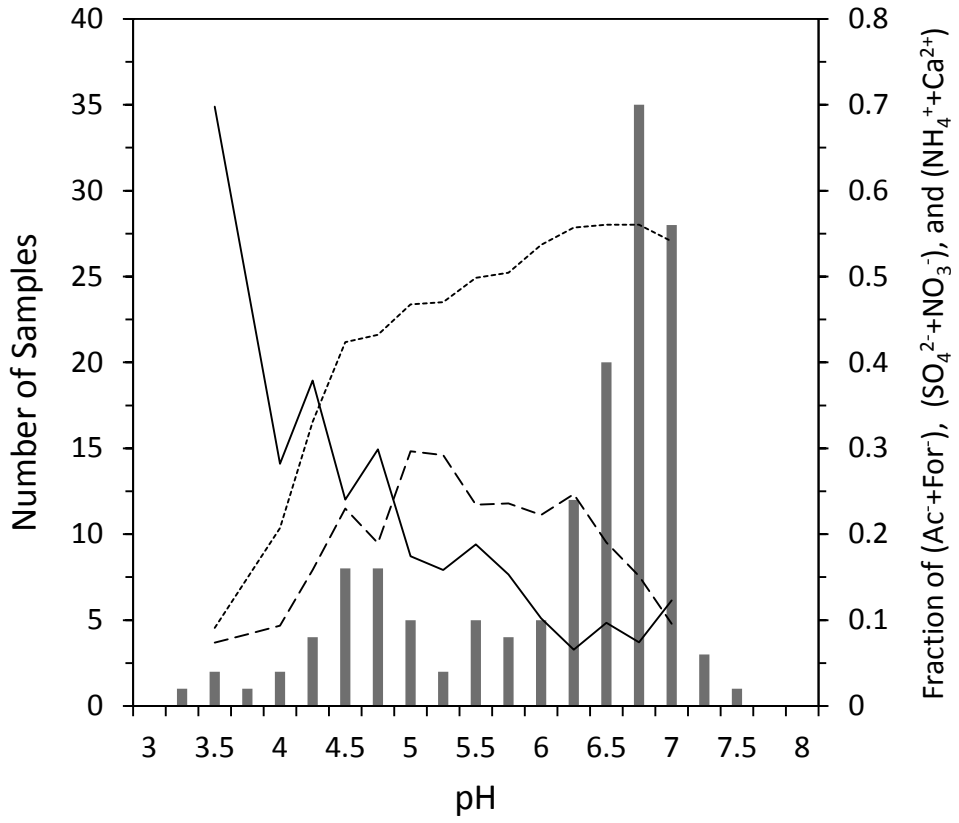

Figure 3. The distribution of pH values for all radiation fog samples (columns). Lines indicate the bin averaged fractions of acetate + formate (solid line), sulfate + nitrate (dashed line), and ammonium + calcium (dotted line) for samples in which organic acids were measured.

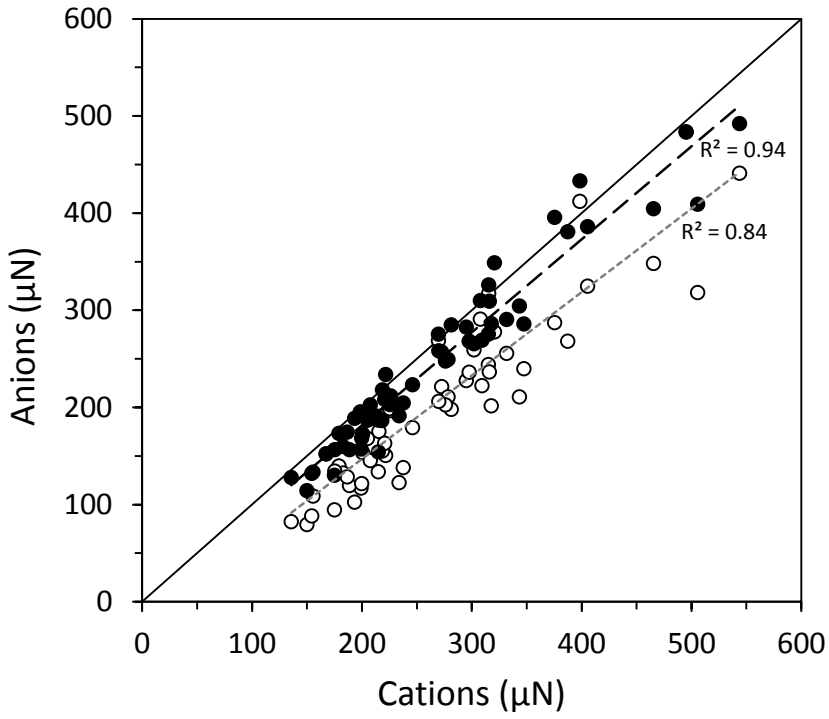

Figure 4. Balance between anions and cations for the subset of fog samples in which TOC analysis was completed (2013 - 2015). Open circles represent measured anions plus calculated bicarbonate in equilibrium with gas phase CO_2. Closed circles represent measured anions plus bicarbonate determined from measured inorganic carbon concentrations.

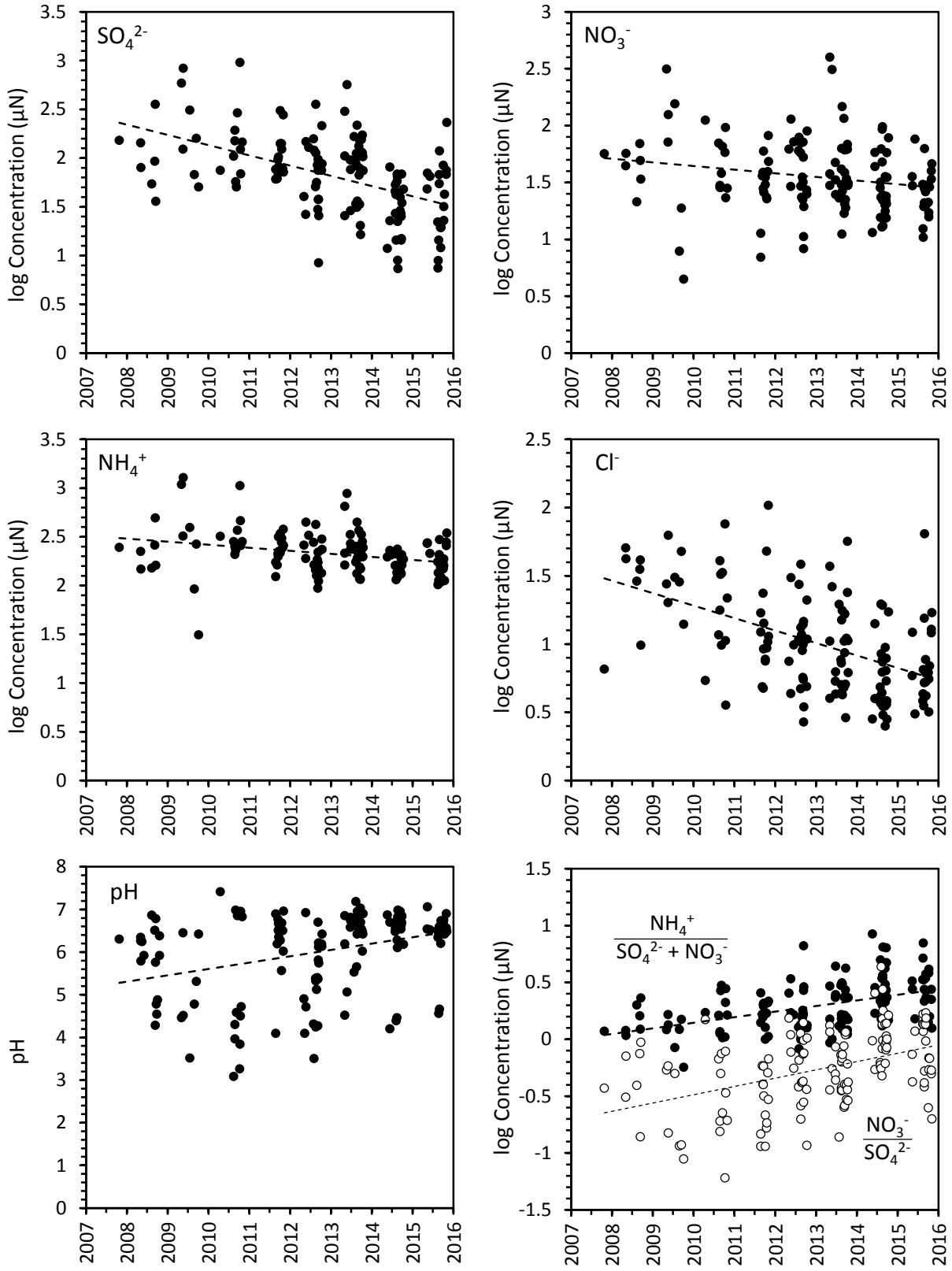

Figure 5. Statistically significant trends in sulfate, nitrate, ammonium, chloride, pH, and the ratios of nitrate/sulfate and ammonium/(sulfate+nitrate) over the duration of the study.

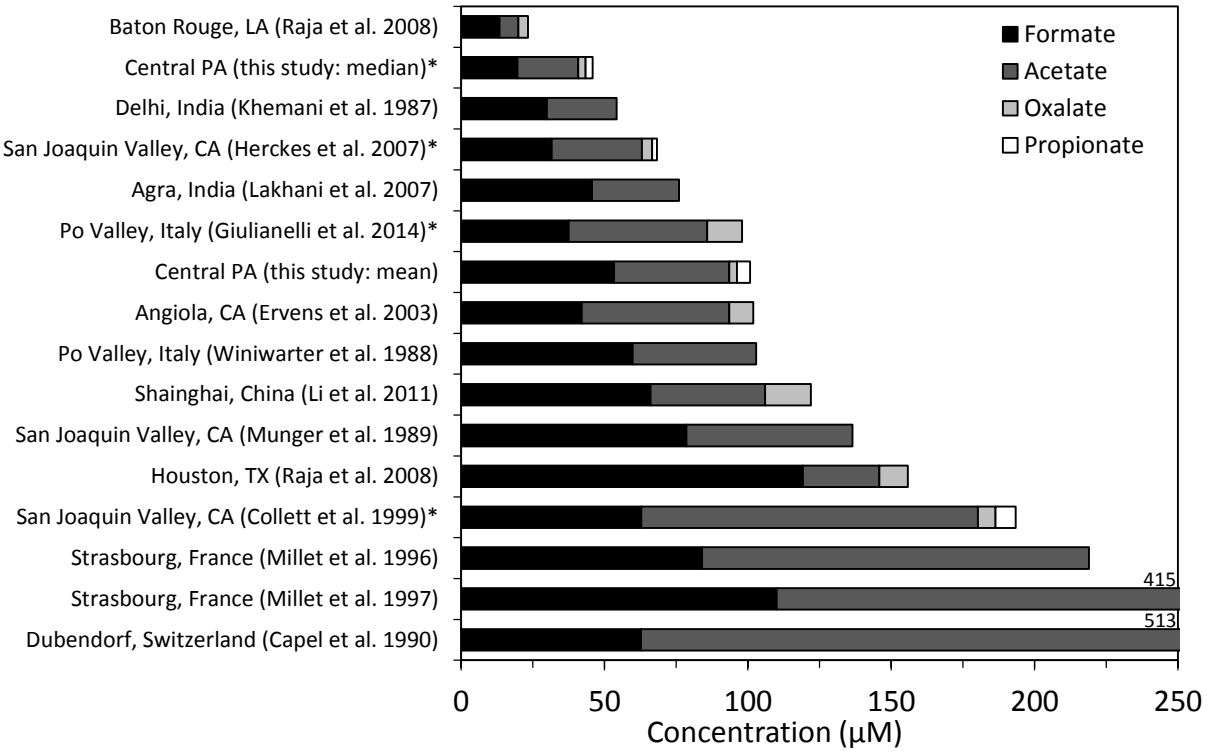

Figure 6. Mean concentrations of formate (black bars), acetate (dark gray bars), oxalate (light gray bars), and propionate (white bars) for the current study in Central Pennsylvania and previous radiation fog studies. Studies that report median values are denoted with an asterisk.

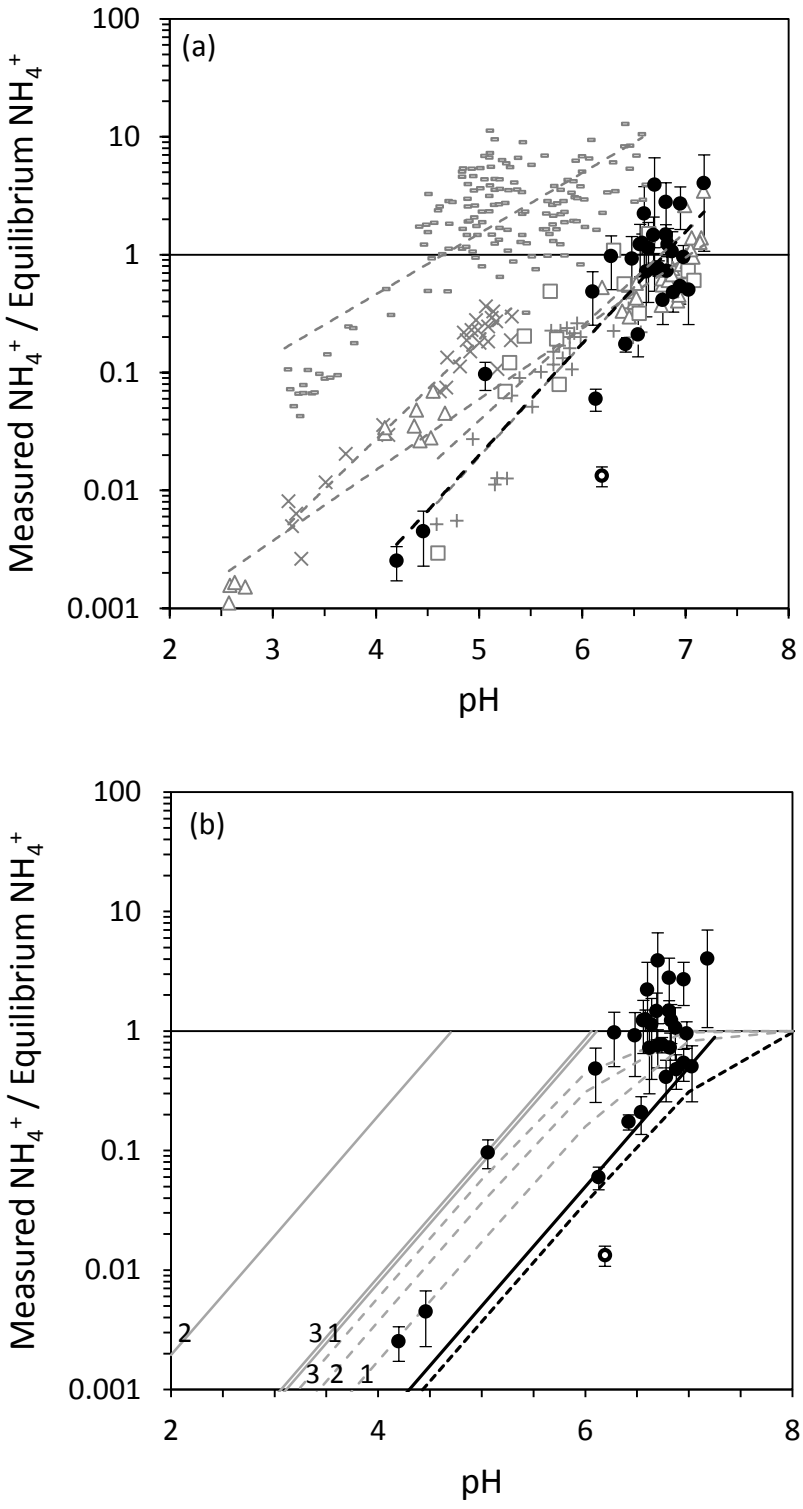

Figure 7. (a) The ratio of measured aqueous phase ammonium concentration to theoretical equilibrium concentration (R_{aq}) for the current study (circles) and from Facchini et al. (1992) (dashes), Winiwarter et al. (1994) (x's), Winiwarter et al. (1994) (pluses), Jaeschke et al. (1998) (triangles), and Jacob et al. (1986) (squares). The open circle represents a sample period in which rime ice was collected during a

supercooled fog event. Error bars for the current study are based on the RSD for ammonium measured in the fog samples and +/- 1.1 ppb for gas phase measurements. (b) Values of R_{aq} for the current study along with modeled R_{aq} values based on derivations by Winiwarter et al. (1994) (solid lines) and Ervens et al. (2003) (dashed lines). The black lines show results for conditions described in Section 3.6 of the text. The gray lines show results for an increase in the accommodation coefficient from 0.001 to 0.01 (1), droplet lifetime from 60 s to 600 s (2), and temperature from 273 K to 295 K (3).